Planetary Mission Preplanning with Heading-Specific Slope and Distance from Shadow

Myles Blodnick
CMU-RI-TR-17-23

Robotics Institute
Carnegie Mellon University
Pittsburgh, Pennsylvania 15213

Abstract

An actual route and terrain for a planetary rover can only be experienced while driving, but preplanning is invaluable to pre-determining route viability. Mission preplanning uses best prior data of terrain topology and lighting for this purpose. A prevailing technique is to compute magnitude of terrain slope at grid points by differentiating elevations of a digital elevation model. Mission planners then threshold on this slope map with a rover's pitch limit to determine whether a location is navigable or not. Traditional grid planning then ensues. This approach is highly restrictive since rovers can side slope on terrain that they cannot climb by direct ascent. All directions other than principal slope can be traversed with less pitch, but incurring some rover side slope. To address the limitation of preplanning on a criterion of maximum slope, this thesis explores planning with consideration of directionality of slope. It accounts for angle of attack at a location, not just amplitude of maximum terrain slope at the location. If a rover approaches a terrain coordinate at the direction of steepest ascent, the pitch required to traverse is the maximum slope of terrain. The planner implemented in this research accounts for the rover's direction of driving on terrain, not just magnitude of maximum terrain slope. Experiments of heading-specific slope planning involved simulated hill and crater terrain as well as lunar data of Nobile Crater. Waypoint destinations unobtainable with non-heading-specific slope planning were possible with heading-specific slope planning. In cases where both types of planning were successful, heading-specific slope planning resulted in a shorter or equal length routes.

Polar navigation poses challenges for solar-powered rovers due to grazing incidences of light. Current planning thresholds on illumination levels of coordinates and binarizes them as lit or unlit. Unlit nodes are then pruned. However, shadow existence and location can't be precisely known due to illumination map uncertainties as well as shadow variance within map timescales. This research implements a distance from shadow constraint that buffers a lighting margin by specifying and computing a euclidean distance away from shadowed nodes. Experiments of distance from shadow restriction planning involved lunar data of Nobile Crater.

Acknowledgments

I would like to thank my advisor, William “Red” Whittaker, for his support and guidance. When I first decided to pursue robotics, I wasn’t sure what I wanted to do nor what I was capable of. Through my time here, you challenged me and helped my development as a student, roboticist, and an individual.

I want to thank Chris Cunningham for introducing me to the research subjects at hand as well as giving me insight into the proper approach to research, Heather Jones for working with me to learn and understand the material, Eugene Fang for helping me understand and analyze the data, Daniel Arnett for helping me prepare the long nights before weekly presentations, and Nate Otten for providing me with the Lunar data used in this research.

To my family: your support helped me stay and push myself to complete this program. To my friends, Josh Kolodny, Anthony Margetic, Bradley Schneider, Michael Wesley Booker II, Jordan Marion, Isaiah Edmonds, Mohammad Ali, Joseph Jung, Anthony DiDonato, Bryant Backus, Jonathan D. Kim, Courtney Pozzi, Lynzky DeLeon, and Joshua Lafazan, you’ve all helped me throughout this process more than you know. Both my individual and academic improvement would not be possible without your assistance. All of your camaraderie made the tough times easy and the fun times even better.

Finally I would like to thank Lebron James for coming back 3-1 in the 2016 NBA Finals. If you could do that, I could finish this Master’s degree. Bryson Tiller, you helped me realize that even when your closest friends count you out, you can push through to success. I would also like to thank the film ‘Superbad’ for helping me laugh through the anxiety caused by this thesis.

1. Introduction

An actual route and terrain for a planetary rover can only be experienced while driving, but preplanning is invaluable to pre-determining route viability. Mission preplanning uses best prior data of terrain topology and lighting for this purpose. A prevailing technique is to compute magnitude of terrain slope at grid points by differentiating elevations of a digital elevation model. Mission planners then threshold on this slope map with a rover's pitch limit to determine whether a location is navigable or not. Traditional grid planning then ensues. This approach is highly restrictive since rovers can side slope on terrain that they cannot climb by direct ascent. All directions other than principal slope can be traversed with less pitch, but incurring some rover side slope. To address the limitation of preplanning on a criterion of maximum slope, this thesis explores planning with consideration of directionality of slope. It accounts for angle of attack at a location, not just amplitude of maximum terrain slope at the location. If a rover approaches a terrain coordinate at the direction of steepest ascent, the pitch required to traverse is the maximum slope of terrain. The planner implemented in this research accounts for the rover's direction of driving on terrain, not just magnitude of maximum terrain slope.

A grid point's maximum slope is calculated by choosing the largest magnitude finite difference of elevations between its neighboring nodes. Non-heading-specific slope planning presumes that a grid point is navigable if its max slope is less than or equal to the rover's pitch ($|slope|_{\max} \leq |pitch_{rover}|$). Each heading on a grid point has a pair of slope and side slope. The slope is calculated by finding the dot product of a vector describing the gradient changes with a vector of the heading direction to a node. Subsequently this is divided by the normalized dot product of the same components. The side slope is calculated with the same process, but with the vector perpendicular to the heading direction. Heading-specific slope presumes a node is navigable if its heading slope is less than or equal to the rover's pitch and its side slope is less than or equal to the rover's roll ($|slope|_{\text{heading}} \leq |pitch_{rover}|$ and $|side\ slope|_{\text{heading}} \leq |roll_{rover}|$).

Fig. 1 shows two completely different routes to the same destination. One is planned with a non-heading-specific (or principal slope magnitude) slope (cyan) and the other with a heading-specific slope (pink), both leading completely different routes from the same starting point to the same destination. The heading-specific slope route navigates over the hill because side sloping on the terrain can reach the summit. The non-heading specific slope route has to circumvent the hill as surmounting would require traversing over terrain with maximum slope values greater than the rovers pitch.

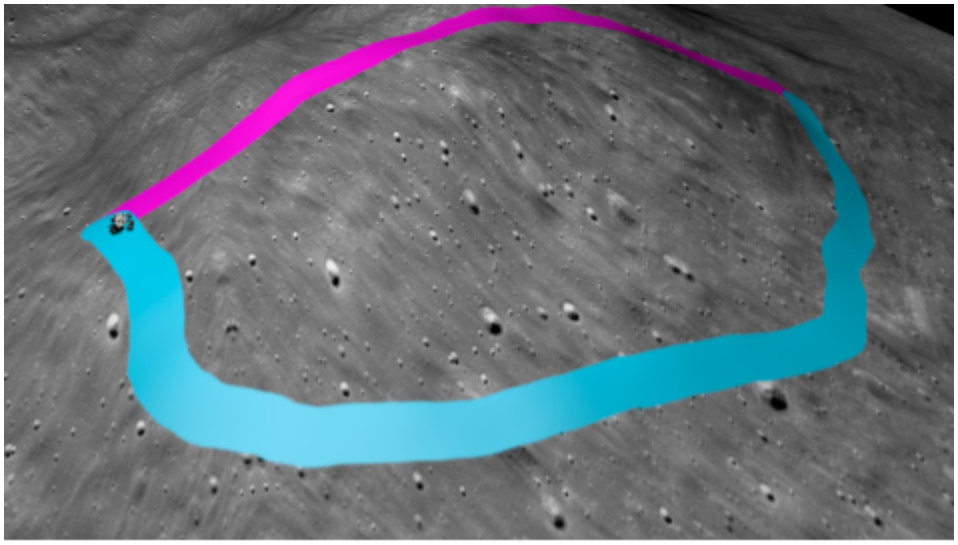

Fig 1: A non-heading-specific slope route (cyan) and a headin-specific slope route (pink) to the same destination

Examples of research planning that utilize maximum slope include TEMPEST and more recent work by Cunningham et al. (Cunningham, C., Amato, J., Jones, H. L. and Whittaker, W. L., 2017). Planning has been implemented to account for route feasibility with heading-specific slope navigation (Howard, Seraji & Werger, 2002) (Karumanchi, Allen, Bailey & Scheding, 2010) (Wellington , C., Courville, A., and Stentz, A., 2006). In prior work, directionality of slope was explored with a traversability index that characterized the terrain feature and its roughness (Howard, Seraji & Werger, 2002) . Other work discussed probabilistic slope modeling from sensor data to determine navigability (Karumanchi, Allen, Bailey & Scheding, 2010) . This research utilizes the principle of directionality of slope on existing terrain data for preplanning.

Ascending out of a crater can be simplified to ascending out of a cone. A cone with slope elevation angle θ (Fig.2) is idealized geometry for the illustrating the principle.

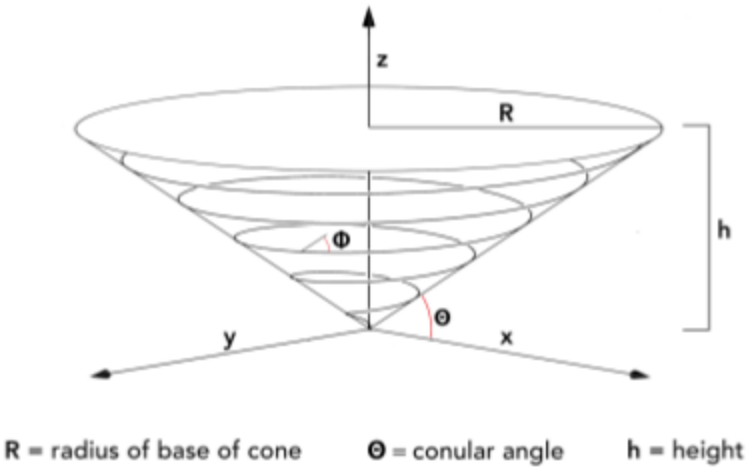

Fig. 2: A a diagram of a spiral around a cone given a multitude of input

If a rover is directly ascending, $\Phi = 0\circ$, θ is the pitch required to ascend and $0\circ$ is the roll required. . If the rover is traveling in a circumferential route, $\Phi = 90\circ$, parallel to the xy-plane, the pitch needed would be $0\circ$ and the roll $90\circ$. S is the length of a spiral out of a cone when t equals the height of the cone. The route is shortest when $\Phi = 0\circ$. The route length increases as it approaches the limit of $90\circ$. It has an infinite route of ascent at $\Phi = 90\circ$. The following equations quantify spiral conical routes:

$\alpha = \frac{2\pi n}{h}$, n= number of spirals

$\phi = \frac{h}{n}$

$Let\ t \in (0, h]$

$x(t) = \left(\frac{t}{h}\right) R\cos(\alpha t)$

$y(t) = \left(\frac{t}{h}\right) R\sin(\alpha t)$

$z(t) = t$

$dx/dt = \frac{R^2\,(\cos(\alpha\, t) - \alpha\, t\sin(\alpha\, t))^2}{h^2}$

$dy/dt = \frac{R^2\,(\sin(\alpha\, t) + \alpha\, t\cos(\alpha\, t))^2}{h^2}$

$dz/dt = 1$

$$S = s(t)\int_0^t \sqrt{\left(\frac{dx^2}{dt} + \frac{dy^2}{dt} + \frac{dz^2}{dt}\right)}\,dt$$

$$S = s(t) = \int_0^t \sqrt{\left(\frac{R^2}{h^2} + \frac{R^2\alpha^2 t^2}{h^2} + 1\right)}\,dt$$

When navigating around geographical features, rovers are exposed to shadows, as designated points of interest may require traveling through shadowed areas. Rovers are challenged with maintaining battery power while navigating hazardous terrain while illumination is changing. Solar illumination is required to maintain power for solar powered rovers. Solar fluctuations also cause drastic swings in temperature which can affect rover operations (Sefton-Nash, E., Siegler, M.A., and Paige, D.A, 2013). Rovers may employ shadow avoidance to sustain solar energy necessary for longer periods of exploration. In addition, remaining in illumination ensures visibility and adequate lighting which is utilized in beacon-based navigation and teleoperation. The second aspect of this thesis regards planning with a distance from shadow restriction (Fig. 3). This mitigates the uncertainty of whether locations at a shadow boundary are actually lit. This increases the certainty that a route preplanned in sunlit will actually be lit while exploring .

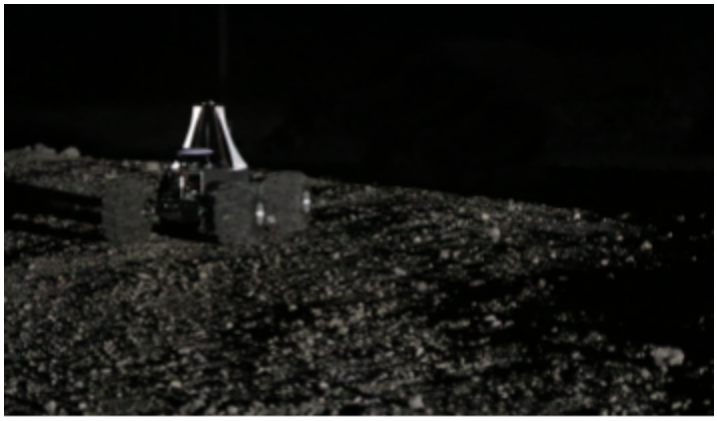

Fig. 3: A rover navigating away from shadowed area

1.1 Terminology

Principal slope of terrain is defined as the maximum gradient of slope along the direction of steepest ascent. This is calculated by computing finite difference between a node and a set of neighbors. The largest finite difference is then selected as the maximum gradient. Distance from shadow is a node's euclidean distance from the nearest non-illuminated node. Roll and pitch are both euler angles. Roll is the angle of rotation on the longitudinal axis; pitch is the angle of rotation on the lateral axis (Fig. 4).

Fig. 4: (Left) a rover's angle describing pitch (Right) a rover's angle describing roll

1.2 Motivation

Craters have numerous navigational factors to consider. A primary factor is the shadowed regions of a crater. Solar powered planetary rovers traversing along a shadow boundary could be prone to shadow exposure. Uncertainties of shadow location may strand rovers in shadowed areas for too long, draining rovers' batteries.

Distance from shadow as well as directionality of slope are applicable in lunar rover navigation. Traversing up steeper slopes requires more battery. However, side sloping routes will be longer. The longer the length of the route, the more a battery depletes. Rovers requiring solar exposure for charging makes exploring areas of scientific interest more difficult. Routes within solar exposure may not be possible with non-heading-specific slope planning. Rovers with a heading-specific slope planner may plan those routes.

Exploring craters with rovers is of scientific interest. NASA's Mineralogy Mapper has collected data indicating that water exists on the polar regions of the moon (NASA, 2012). On the lunar equator, the impact crater Ballialdus is of high interest to scientists because of its location as well as a rock material in its central peak that is formed within the crust and mantle (NASA, 2010). Therefore, the possibility of best finding water on the lunar terrain requires navigating a crater. In a crater, shadow exposure and principal slope of terrain exceeding rovers' capabilities are common issues, both of which this research addresses.

1.3 Contributions

1. The first contribution is incorporating roll and pitch capabilities into a planning algorithm.

2. The second contribution is a distance from shadow feature so a rover can traverse in sun-synchronous regions, limiting shadow vulnerability.

Although autonomous rover path planning software exists, these two factors have not been adequately addressed yet.

2. Background

2.1 Rover Planning

This section first discusses methods for generating deterministic plans on search graphs. It then expands into constraint planning before focusing on the specific constraint of solar-planning.

2.1.1 Graph-Based Planning

Graph-based methods are a path planning staple (Even, 2011). Dijkstra's algorithm is a standard. It is always complete, meaning it will always find a solution and that solution will always be the shortest path possible. The algorithm functions to find the shortest path between a source node and all other nodes on a graph, utilizing a priority queue (Dijkstra, 1959). The algorithm takes inputs from nodes; as nodes are expanded, they are added to the queue and the queue is adjusted accordingly. Therefore, the search radiates outward along the shortest possible paths given the priority of the nodes. Dijkstra's algorithm is the best and most complete formula to use, however, it is slow to compute. It makes no assumptions about its environment and will often expand many more nodes than are necessary—expanding equidistant in every direction.

Runtime can be reduced if heuristics are applied such as manhattan distance, euclidean distance, etc. This can be done without sacrificing optimality (Haslum & Geffner, 2010). This is very similar in strategy to the A* planning algorithm, which utilizes a heuristic to act as an estimate of the final cost to reach a goal from any node (Hart, P.E., Nilsson, N.J., and Raphael B., 1968). Therefore, node expansion occurs in the direction of the goal rather than uniformly from the starting location. The preconditions are that the heuristic must be admissible and consistent.

The A* algorithm, while over 50 years old, has seen some modernization. For example, Phillips parallelized the neighbor state expansion stage; and very recently, the use of multiple heuristics has become popular—allowing for heuristics to have their own priority queues and update in real time when a better path is found, given any of the heuristics—this significantly speeds up search time when multiple factors and differentiations are present (Phillips, Likhachev and Koenig, 2014).

2.1.2 Constraint Planning

Work with constraint planning utilizes risk and resource factors. For example, the Mixed-Initiative Activity Plan Generator (MAPGEN) is used as the planner scheduler for the MER mission (Sanders et al., 2005). Furthermore, constraint planners are common on Mars-based rover missions. MSL uses MSLICE (Mars Science Laboratory Interface) and RSVP (Robot Sequencing and Visualization Program) to schedule tasks and enforce constraints (Cunningham, Johns, Kay, Peterson & Whittaker, 2014) . Some constraint planners involve humans identifying designated waypoints of interest and the resource constrained-planner finding feasible routes that reach them.

Resource-constrained planning has utilized risk factors, such as energy modeling, slope levels, solar exposure, ect., when generating these routes. The most notable of these planners is TEMPEST (Temporal Mission Planner for the Exploration of Shadowed Terrain)(Tompkins, 2005). The utilization of shadow maps by TEMPEST allowed for sun-synchronous navigation paths that optimized energy constraints. In addition, it used slope elevation as a factor for energy constraints. Higher slope terrain required more battery discharge to power the motors and ascend the rovers up inclines.

A set of time-discretized maps have been utilized in resource constrained planning when assigning shadow values as solar exposure varies in a time sequence (Cunningham et al., 2014). The time interval duration of each map is small enough that no significant changes appear in an area location over adjacent time indexes.

While planning has limited rover movement in constrained areas, more could be done to further ensure the safety of a rover. It would be more ideal to navigate within a lit region rather than along the shadow boundary when identifying safer paths that still meet the resource constraints.

2.1.3 Solar Planning

Sun-synchronous navigation formally started with K. Shillcut's "Solar Based Navigation for Robotic Explorers"(Shillicut, 2000). Traveling along sun-synchronous paths enables continuous activity (Whittaker, W. L., Kantor, G., Shamah, B., and Wettergreen, D, 2000). Shillcut's work also discusses how solar navigation can find the nearest sunlit spot for recharging and determine how long said spot will remain lit. Shadow maps are precomputed in order to determine solar-based navigation (Otten et al., 2015). The shadow maps use an 8-connected propagation search on two-dimensional terrain space, starting from a given grid cell and time.

In space robotics, solar-centric path navigation is common. One of the more notable examples of sun-synchronous navigation is Hyperion. Hyperion was developed as a polar rover for reduced

mass, reduced complexity, and vertically-oriented solar panels (Wettergreen et al., 2002) . The rover was designed to negotiate terrain features to avoid shadowing and remain in unobstructed sunlight to store power enroute. Hyperion's main challenges involved optimizing the orientation of its solar panel with respect to the sun (Tompkins, Stentz & Whittaker, 2002). This optimization meant that ability in path planning had to factor in avoiding obstacles and reaching goal locations as well as maintaining a preferred orientation all the while. It was noted in Hyperion's first experiment, that the robot can fall behind if rough terrain is encountered but enough power margin helped regain the scheduled plan. Although the robot was able to autonomously navigate to waypoints and avoid obstacles, but teleoperation was required in rough terrain (Teti, F. , Whittaker, W. L., Kherat, S., Barfoot, T., and Sallaberger, C, 2005). However, the ability to operate the sun-synchronous and maintain the necessary power levels was clearly demonstrated.

2.2 Navigating Terrain Features

This section focuses on mechanical designs to react to terrain features before addressing former research in roll and pitch capability.

2.2.1 Mechanics of Roll and Pitch Capability

The fundamental criteria for tip-over stability is that to achieve static stability, the center of gravity must lie above the convex area (support polygon) spanned by the ground contact points (McGhee & Frank, 1968). If a rover's center of gravity falls outside its support polygon, the rover tips over. Further, the magnitude of the static stability margin for an arbitrary support polygon is equal to the shortest distance from the vertical projection of the center of gravity to any point on the boundary of the support polygon (McGhee & Frank, 1968). As the height of a rover's center of gravity increases, the tipover stability margin decreases. At a zero elevation of height, it slips until it reaches its slip limit before tipping over.

In this research pitch and roll capability relate to the ability to drive. The angular limits of driving are bounded by the angular limits of tipover stability. More specifically, the first condition is for a rover to be statically stable when sitting on terrain and those capabilities for static stability always exceed a robot's ability to climb and drive. A rover's pitch capability is its ability to drive/climb and its margin to not tip. A rover's roll capability is its margin relative to falling over. Both have to be less than or equal to tipover stability.

Chassis design has sought to maximize steep driving and tipover margin. Icebreaker was designed with a low center of gravity to overcome steep slopes and side-slope navigation (Ziglar, 2007). Further, Adjustable chasse have enabled rovers to maximize stability by shifting the

center of gravity. Feedback control allows an actively reconfigurable chassis to adjust configurations to maximize the stability of the rover (Tarokh & McDermott, 2005). Reconfigurable rovers can improve pitch and roll driving and stability in rough terrain by repositioning their center of mass (M. Tarokh & G. McDermott, 2007).

The Jet Propulsion Laboratory's Sample Return Rover (SSR) (Fig. 5) and Carnegie Mellon's Scarab (Fig. 6) were designed for improved ability to ascend and descend side slope. When traversing an incline SRR can lower one side of its suspension and reposition its manipulator to redistribute its center of mass and bolster stability. Moving the rover's center of mass reduced motor torques and energy consumption while maintaining stability and terrain adhesion (Nakamura et al., 2007). Scarab and the Sample Return Rover both can independently set their sidearm angle to adjust their independent chassis wheel bases (Iagnemma et al., 2000) . Reactive control on the sidearm of the rover's sidearm maximizes the stability (Schenker et al., 2000). This enables posturing of the robot body with actively adjustable wheel bases that are not possible with fixed chassis robots.

Fig. 5: SSR performing cliff traversal (Jet Propulsion Lab)

Fig. 6: Scarab side-sloping a terrain feature (Kohanbash)

The Model Predictive Control system has been developed for model predictive control of vehicle posture. This system improved rovers' performances while traversing slopes, specifically Scarab (Fig. 7) (Furlong, 2009). Although a purely reactive system outperforms the model predictive approach in terms of minimizing roll, no work was done with reactive system planning.

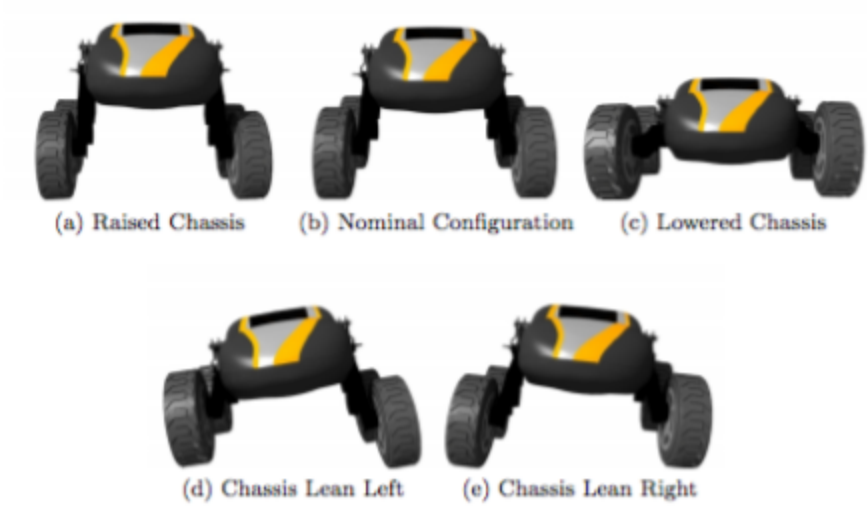

Fig. 7: Articulation capabilities of the Scarab mobile robot. Symmetrical values for the sidearm chassis angles enables the body to raised (a) to avoid small obstacles or lowered (c) to reduce the risk of tip over. Asymmetrical sidearm chassis angles enables the body to be postured left (d) and right (e) to achieve more stable configurations on rocks and slopes (Furlong, 2009)

Mechanics of roll and pitch capability were explored as roll capability requires a different mechanical design than pitch capability alone.

2.2.2 Heading-Specific Slope Planning

The polar path planner utilizes the principal slope of a terrain coordinate in terms of doing slope thresholding (Cunningham et al., 2014). This technique is considered safe—it ensures that the rover will traverse a terrain regardless of the direction it approaches it from.

Plowing strategy for direct descent has shown the possibility of minimizing slip in direct descent. (Ziglar, J., Kohanbash, D., Wettergreen, D., and Whittaker, W. L., 2007). Displacement from a starting point to target destination was low with plowing. (Ziglar, J., Kohanbash, D., Wettergreen, D., and Whittaker, W. L., 2008). The slip control system that was implemented for direct descent reduced slip levels for different grades of terrains, which shows there is a possibility for precise down-slope movement on slopes up to 31° in planetary rovers (Lemus, Kohanbash,. Moreland & Wettergreen, 2009). Furthermore, the fact that the plow had a small down-slope displacement during point-turning is indicative of the possibility of effective in-place turning at maximum depths (Wettergreen et al., 2009).

It is widely believed that for most slopes, the highest possible direct ascent angle will result in the shortest distance, and therefore the most efficient, path (Inotsume, 2015). However, on high slope terrain, slip approaches 100% when rovers directly ascend. In these high slopes, rovers perform better diagonally up a slope than direct ascent, in regards to wheel slippage (Ziglar, J., 2007). This is useful in lunar navigation scenarios, such as rovers ascending out of craters (Fig. 8). Therefore, depending on the heading direction, the rover's navigation may have better performance in slip reduction using the cross-slope of a terrain (Inotsume, Creager, Wettergreen & Whittaker, 2016)

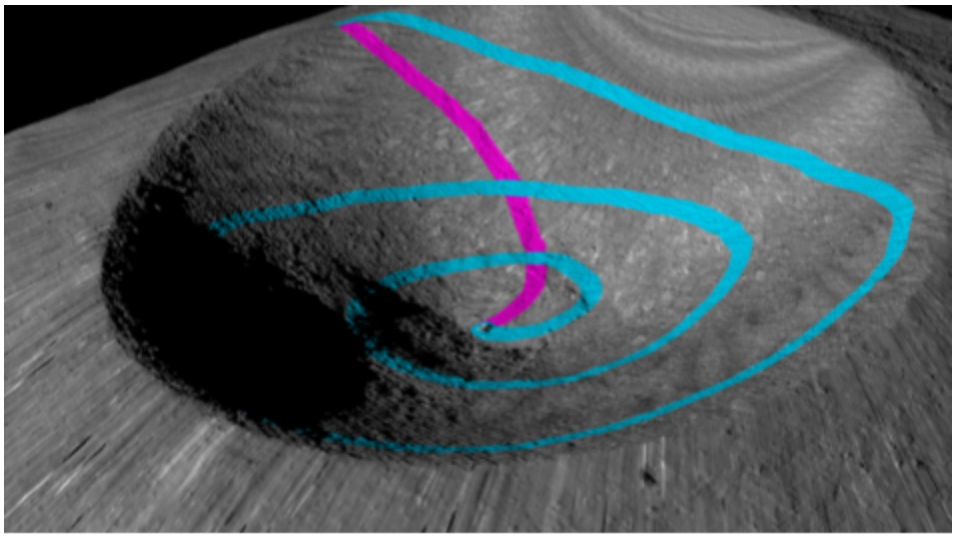

Fig. 8: Pitch-only capability (pink) rover and Roll and Pitch capability (cyan) ascending out of a crater

Scene interpretation from images, such as navigating the terrain depending on the rover's direction, can lead to different slope gradients (Karumanchi, Allen, Bailey & Scheding, 2010). Querying on these different gradients can lead to different traversability maps for navigating around obstacles. This does not involve calculating heading direction as this requires real-time querying on images (Howard, Seraji & Werger, 2002).

2.3 Summary

Rover performance on a mission can be jeopardized when in complex environments. Previous operations have shown that planning for certain constraints when generating an optimal path can still result in the deterioration of rovers' battery or place rovers in a positions where they become immobile.

Resource constrained planners have factored in time-synchronous maps for performing sun-synchronous planning. They have also factored in slope levels to ensure rovers' success, but have not planned for different angles that may help rovers to better navigate complex terrain.

3. Methodology

This methodology assumes a flat rover.

3.1 Roll and Pitch Capabilities

Roll and pitch capabilities are a static feature for not falling over and driving respectively. Therefore, a path can be optimized by removing nodes that exceed a rover's roll or pitch capabilities, preventing those nodes from being explored. However, the calculation of slope and side slope needs to occur based on the heading direction of the rover. For each node in the graph, there must be a mapping to sixteen nodes to represent each heading direction. The angles of heading direction include:
$0\circ,\ 22.5\circ,\ 45\circ,\ 67.5\circ,\ 90\circ,\ 112.5\circ, 135\circ,\ 167.5\circ,\ 180\circ,\ 202.5\circ,\ 225\circ,\ 247.5\circ,\ 270\circ,$
$292.5\circ,\ 315\circ\ \&\ 337.5\circ.$
Each angle is represented in vector form.
The first step in this process involves calculating slope and side slope and can be described directly as:

h = *heading direction vector*
s = *side direction vector*
$\triangle F_x$ = *Gradient in X direction*
$\triangle F_y$ = *Gradient in Y direction*
u = *side slope*
v = *slope*

$$s = h^{\perp}$$
$$m = [\ [\triangle F_x,\ \triangle F_{y,}\ \triangle F_z\ ] \bullet s] \ /\ \left|[\triangle F_x,\ \triangle F_{y,}\ \triangle F_z]\right| |s\ |$$
$$u = cos^{-1}(m) - \frac{\Pi}{2}$$
$$n = [\ [\triangle F_x,\ \triangle F_{y,}\ \triangle F_z] \bullet h] \ /\ \left|[\triangle F_x,\ \triangle F_{y,}\ \triangle F_z]\right| |h\ |$$
$$v = cos^{-1}(n) - \frac{\Pi}{2}$$

The next step in the process is to traverse the terrain map for each heading direction, filtering each spot as a valid location based on roll and pitch capabilities. Subsequently, each heading direction terrain map is turned into a graph of valid nodes—only those with edge connections to neighbors that are valid in that heading direction. Nodes are considered valid if they meet they are within roll and pitch capabilities. If not, they are pruned off. Then, the valid node graphs are all composed to form a new multi edge graph so that each node is then reachable based on changing heading direction. Now, planning can be done whereby going from node to node has a cost of x, but rotating to changing heading direction has a negligible cost. For comparison, planning without direction assumes approach at the worst orientation and therefore pitch is the threshold.

3.2 Distance From Shadow

The presence of shadows in lunar environments serves as a major hazard for rovers. The amount of shadow present in a region places further difficulties on rovers that are solar powered. Darker regions, areas of lower incidence of light, place rovers at an increased risk for electronic malfunction because of low temperatures (Vasavada et al., 2012). They also force rovers to utilize non-vision sensing in order to traverse terrain safely.

Because of the difficulties regarding lunar shadows, experiments are conducted utilizing both hard and soft thresholds. Rovers with a high threshold and a lower-penalty soft threshold on the amount of shadow will be perfectly capable and inclined to traverse permanently dark areas within craters, whereas a low hard threshold will always tend towards traveling the safe regions of the moon, as they have less shadows.

The overall technique behind the euclidean metric for distance from shadow value was calculated by doing a distance transform of the binary image of the illumination map. For each pixel in the illumination map, the distance transform assigns a number that is the distance between that pixel and the nearest zero (unlit) pixel of the illumination map (Fig. 9).

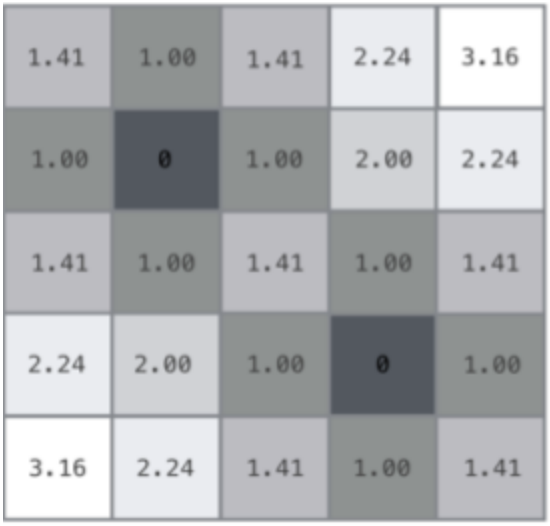

Fig. 9: A distance from shadow calculation on a larger illumination map

As illumination maps change, a multi-edge graph for distance from shadow changes to account for time intervals. This is done by switching the node value cost as the length of the path exceeds a designated value. Therefore each node has multiple distance of shadow values. The value that is determined depends on the path length before accessing the node. For this approach, it is assumed that traveling a set distance will always take the same amount of time to complete. This method also assumes that there is a maximum path length obtainable in a time interval.

3.3 Metrics

The most important metric to utilize when determining path is the universal standard for which path is the shortest. For this research, the path length was measured in meters (m). The best and easiest path is often that which requires the least amount of work by the robot, which often correlates directly into that which takes either the least distance or time. However, this is not always the case in lunar exploration, as the goal is not solely accurate and efficient movement, but area exploration. Therefore, when path planning rovers, the hazard capabilities and battery consumption must be taken into account. On moon terrain, the shortest path is best is when rovers have high hazard capabilities and are capable of surmounting more difficult terrain that less-capable rovers would circumvent.

Therefore, determining the validity of distance from shadow constraints, accuracy of distance from shadow can be checked using distance from shadow and whether or not the outcomes correctly map to terrain features such as elevation peaks or craters. For heading-specific slope planning, there are several ways to measure this constraint. One technique is to see if more valid paths are created when compared to navigating over absolute slope magnitude. Additionally,

path length can be considered because heading-specific slope planning should make more nodes traversable.

4. Results

4.1 Heading-Specific Slope Planning Simulation

4.1.1 Simulated Crater and Hill Terrains

It is useful to plan and navigate over terrain that would otherwise be impossible via non-heading-specific slope planning. The ideal situation for this type of navigation involves craters and hills. In a crater simulation (Fig. 10), there are two main route types: descent and ascent. If rovers are placed into the center of a basin, they would not plan in a direct descent due to high levels of longitudinal slip. Therefore, a rover with a $10 \circ$ roll and a $5 \circ$ pitch capability was selected to ascend as the rover would experience less longitudinal slip compared to a rover with a higher pitch capability. The result is seen in Fig. 12 (pink path), where the rover makes a series or diagonal ascents at various angles of approach that mimic a spiraling route. However, if rovers were to attempt to descend into the crater, slip is more likely to occur the longer the route, causing rovers to stray from the target waypoint in the basin. In this case, direct descent is the more favorable navigational approach. Therefore, a rover with a $5 \circ$ roll and a $10 \circ$ pitch capability was selected to descend as this resulted in a more direct route and slip wa not as much of a concern for descent. The result is seen in Fig. 11 (cyan Path), where the rover's path resembles a nearly straight line

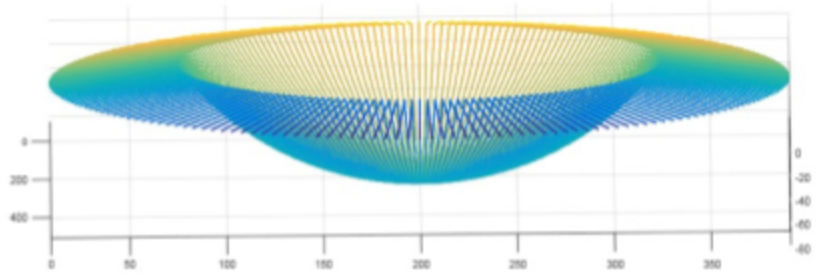

Fig. 10: A 3D perspective of a simulated crater terrain

.

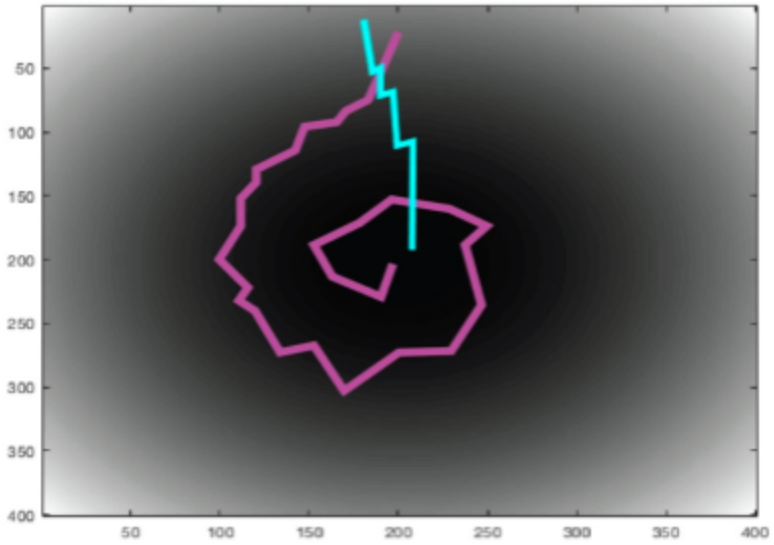

Fig. 11: (Pink) Rover with 15 deg roll, 5 deg pitch capability ascending out of a crater; (Cyan) Rover with 5 deg roll, 15 deg pitch capability descending into a crater;

The area simulated was a hill terrain which is seen in Fig. 12. The benefit of this terrain simulation was that both non-heading-specific slope planning and heading-specific slope planning were capable of operation on this type of terrain feature. Two types of route planning were explored: 1) navigating to a target waypoint on the hill, and 2) navigating to a waypoint where the hill is an obstacle in the route of the true shortest path.

In the case of navigating to a target waypoint, the biggest difference emerges when a waypoint is selected which exceeds a rover's maximum slope capability. As seen in Fig. 13 route A, a route that accounted for both roll and pitch capabilities successfully ascended the hill while the non-heading-specific slope planner could not find any routes that didn't exceed its maximum slope. With regards to navigating around the hill, the heading-specific slope route was significantly shorter than that of the rover that planned with non-heading-specific slope. In routes B and C, it can be seen that the rover that employs heading-specific slope planning navigates in a mixed curvature motion much more closely to the true euclidean shortest distance.

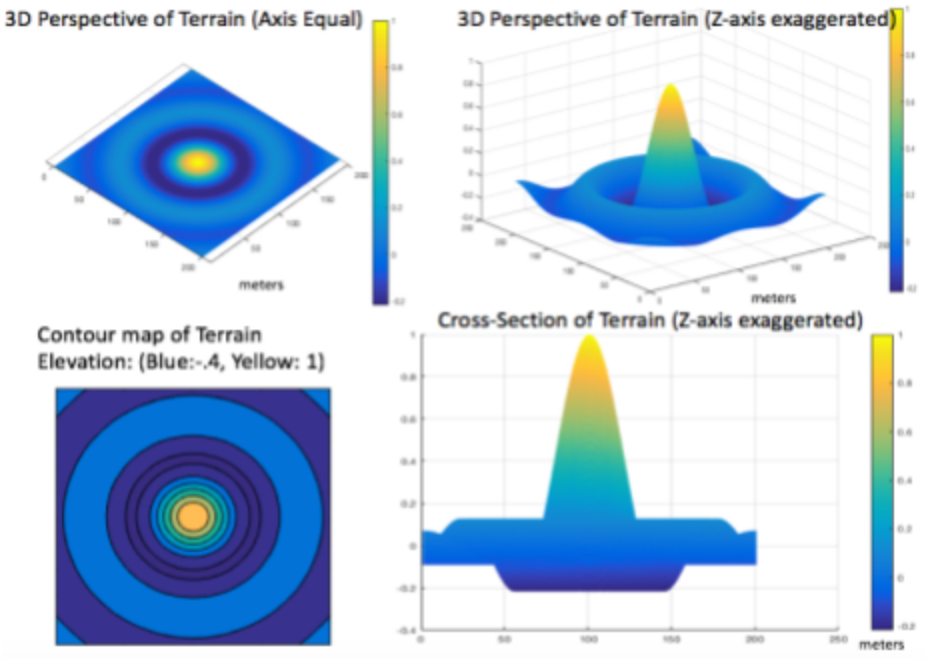

Fig. 12: Four various depictions of the simulated hill terrain

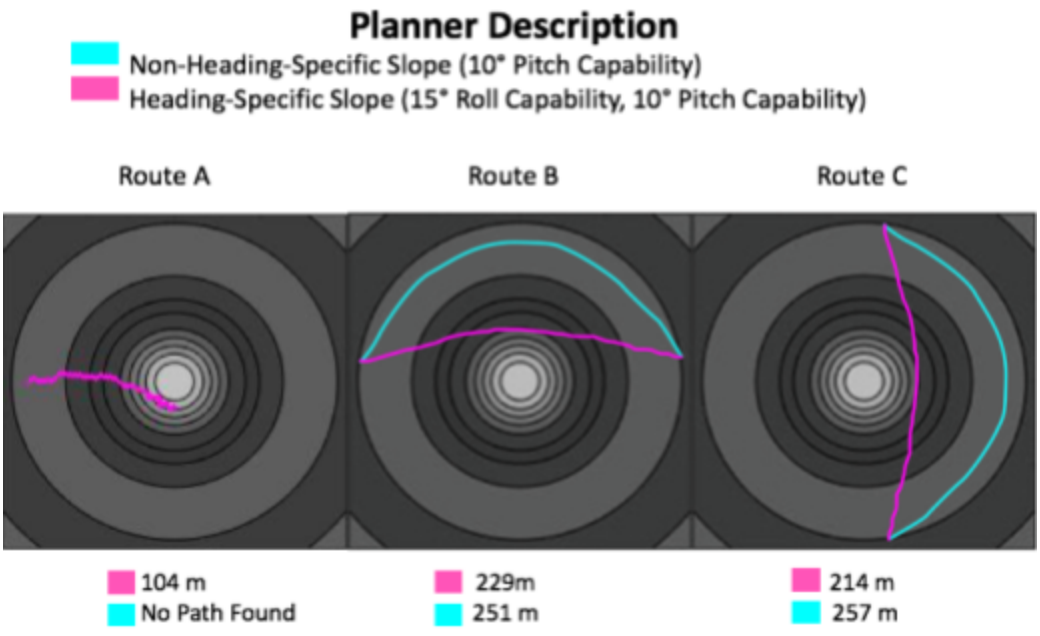

Fig. 13: Two rovers, utilizing different planners, planning three routes to designated waypoints

Roll and pitch capability variance were examined further through rover simulations. Fig. 14 shows varying roll capability with a constant pitch capability. The results showed that as roll capability increases, the path tends to result in a straighter spiral motion. Fig. 15 shows varying pitch capability with a constant roll capability. The results from this simulation show increasing pitch capability increases the ability to perform jagged ascents across the hill. In both cases,

increasing the capability levels allow rovers to travel in a shorter length path to the target waypoint. Low roll and high pitch capability should be utilized for planning on finer terrain which causes longitudinal slip, while high roll and low pitch capability would have more benefits on coarser terrain (Kohanbash, 2017).

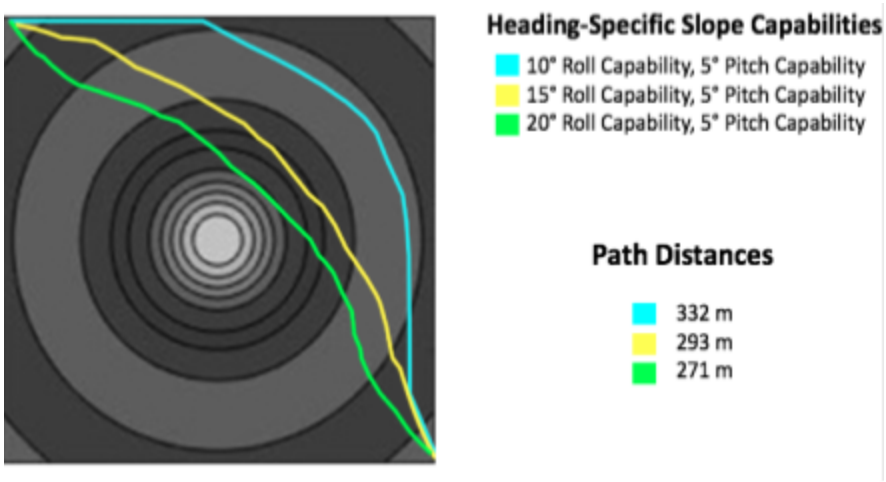

Fig. 14: Multiple rovers with varying roll capability and constant pitch capability planning routes

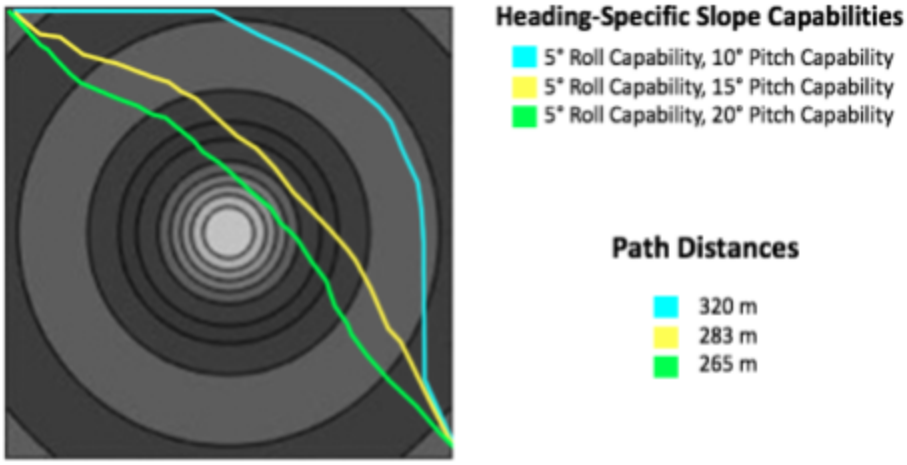

Fig. 15: Multiple rovers with constant roll capability and varying pitch capability planning routes

The results of these paths show pitch and roll capability variance affects path and rovers' capability to reach exploration targets. To see if these effects held, a more complex terrain (series of craters and hills) was modeled (Fig. 16). In Fig. 17, a total of five paths were modeled. The pink path, which correlates to the rover with non-heading-specific slope planning, has the longest path compared to the euclidean shortest distance path (red path). For the remaining rovers with varying roll and constant pitch capabilities, the highest roll capability (green path) had the

shortest path distance. The lowest roll capable rover (cyan path) had the longest path of the heading-specific slope planned rovers.

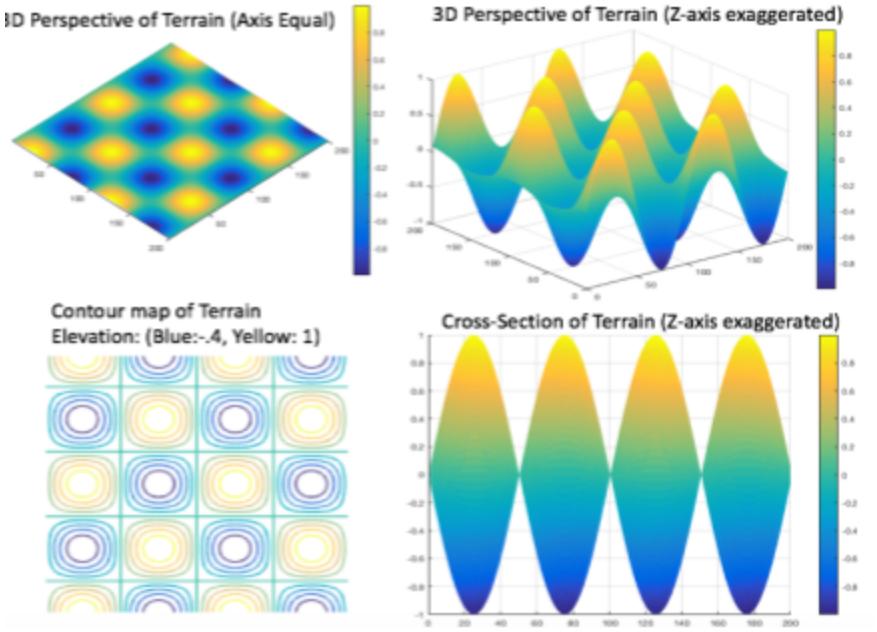

Fig. 16: Four various depictions of the complex terrain simulation

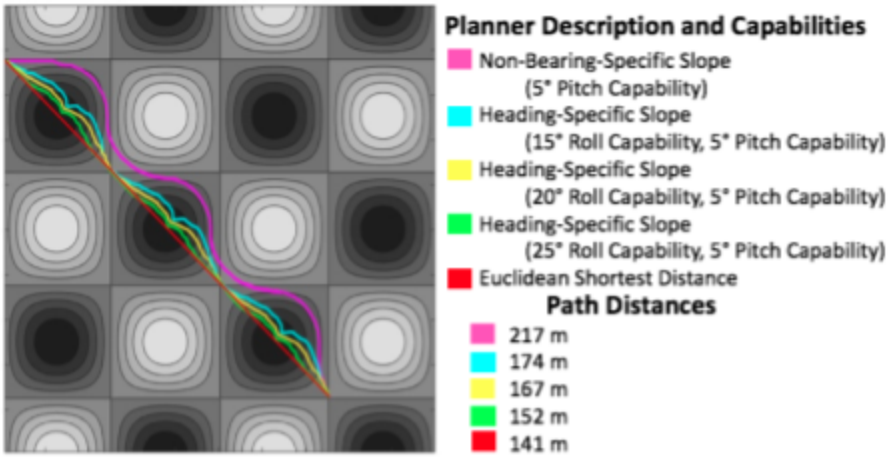

Fig. 17: Five rovers planning with different capability requirements. The routes are planned over a terrain composed of craters and hills.

4.1.2 Simulated Nobile Navigation

Nobile (Fig. 18) is a crater that is located near the southern pole of the Moon. It is an eroded crater formation cloaked in shadows, but has sunlight penetration at oblique angles. The crater rim is overlaid by several lesser craters, most notably on the western rim. This results in principal slope levels that exceed 20◦ while most planners limit rover pitch capabilities to below that. Thus, it may be possible to ascend the crater rim through planning with heading-specific slope.

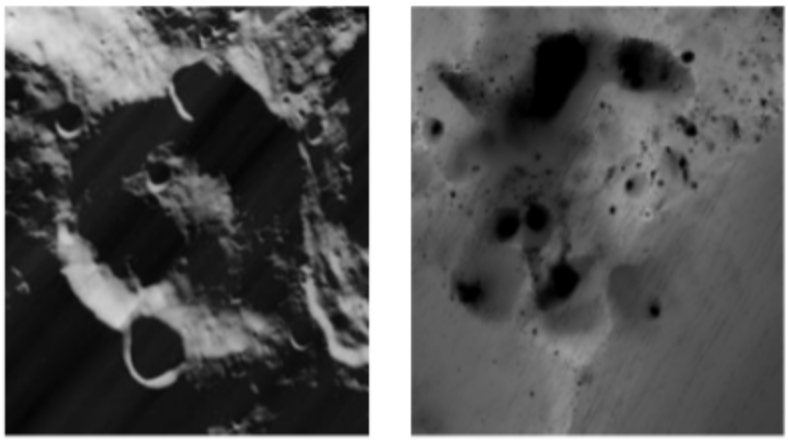

a) An image of Nobile b) Nobile illumination map

Fig. 1: Two images of Nobile

Two areas of Nobile were explored for the testing implementation of heading-specific slope planning: the Northwestern and the Western rims. In the Northwestern rim (Fig. 19), traveling along the rim is seen as possible and to have little impact (Fig. 20a Route A & B) as both the rover with non-heading-specific slope planning and the rover with heading-specific slope have almost no difference. However, when the rovers try to ascend out of the crater, only the rovers with with heading-specific slope planning ascended out of the crater (Fig. 20a Route C & D). Fig 20b shows routes C and D planning on a principal slope thresholded map to show why non-heading-specific slope planning is impossible

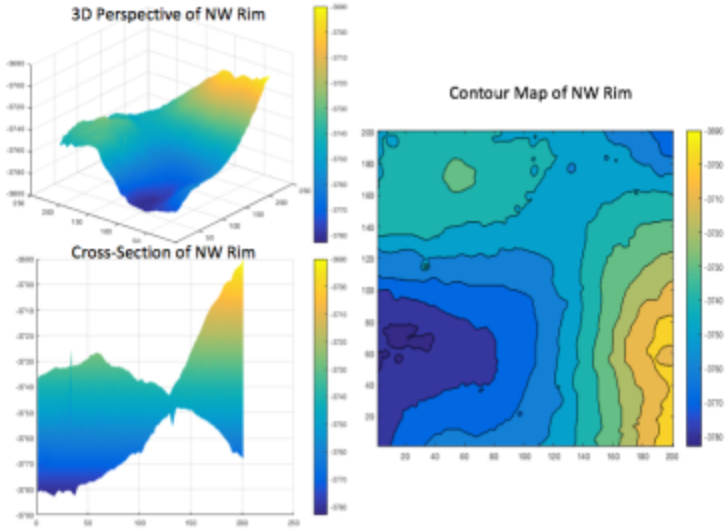

Fig. 19: Three different renderings of Nobile's northwestern rim

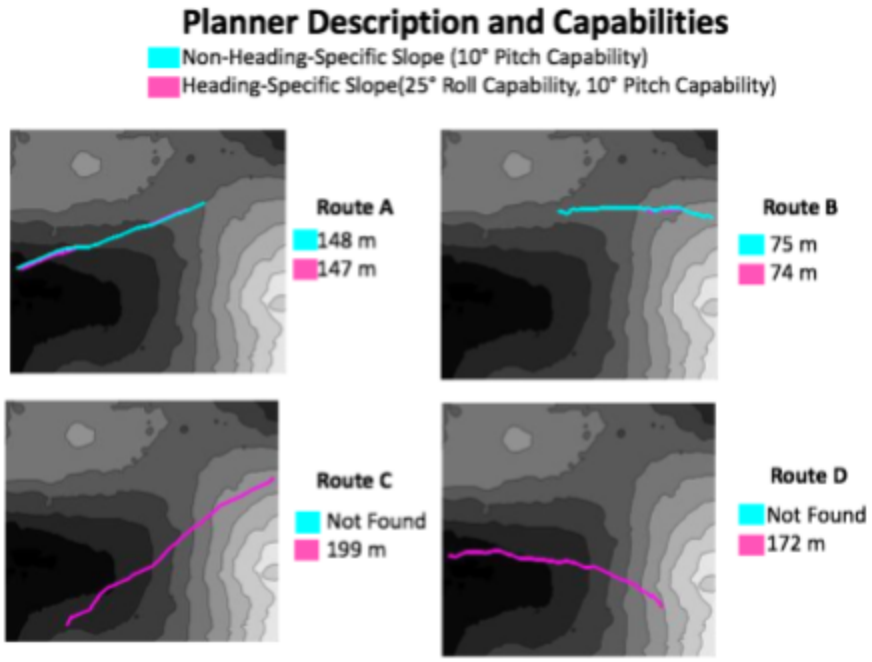

Fig. 20a: Two rovers using two different planners for four different routes

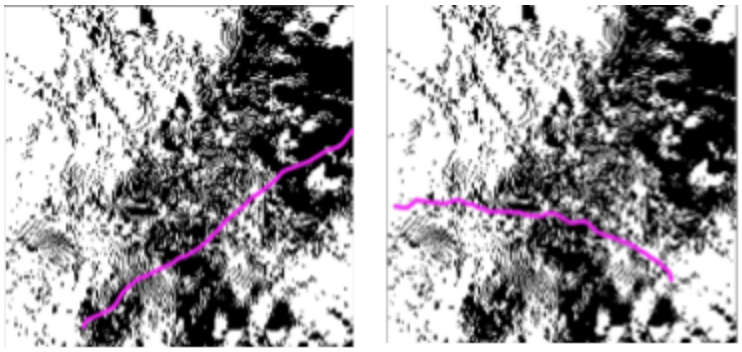

Fig. 20b: Routes C and D on a principal slope thresholded map

Path simulation along the western rim (Fig. 21) shows a bigger differentiation in path length when non-heading-specific slope planning as well as heading-specific slope planning are possible. Fig. 22 (Route B) shows that the pitch-capable rover navigates around a mini craterlet for a path length of 41m, while the rover with heading-specific slope planning descended and ascended out of the craterlet for a path length of 2m. However, when ascending over most of the rim, only the rover with heading-specific slope planning found a path (Fig. 22 Routes C and D).

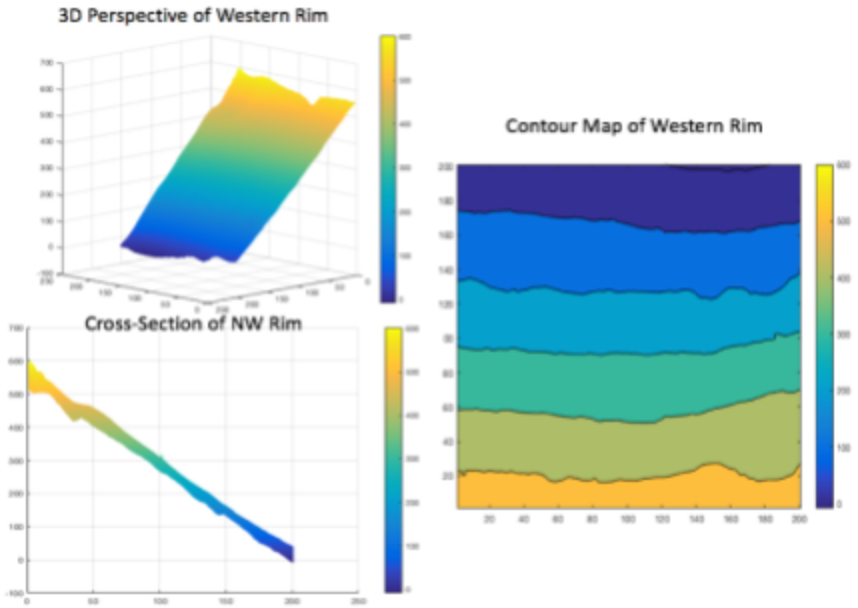

Fig. 21: Three different renderings of Nobile's Western Rim

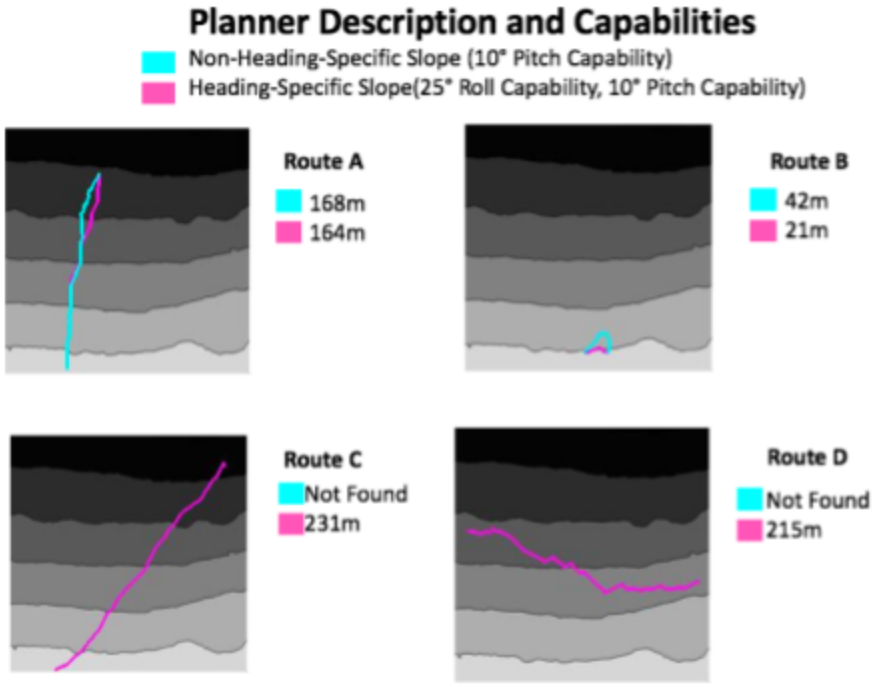

Fig. 22: Two rovers using two different planners for four different routes

4.2 Distance from Shadow Simulation

The area examined was the southwestern rim of Nobile (Fig. 23). This subsection of Nobile exceeds principal slope levels of 20 ◦ and has sunlight penetration at oblique angles. This allows navigation into areas that are usually covered in lunar shadow.

In Fig. 24, two rovers planning with non-heading-specific slope were simulated for two different routes. In Route A, the shadow restriction added a 77m increment, which suggests that this distance from shadow constraint significantly alters the path. Similar results are seen in Route B, where the distance from shadow restriction increased the path by 12m. However, lengthening the path cannot be determined as a negative impact as the restricted rover is less likely to have electronic degradation due to temperature, as well as remain with more battery capacity.

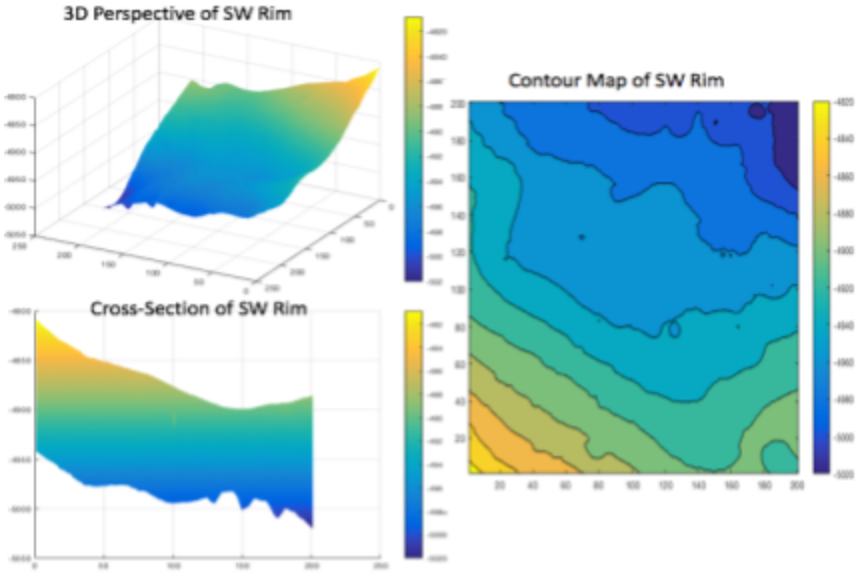

Fig. 23: Three different renderings of Nobile's southwestern rim

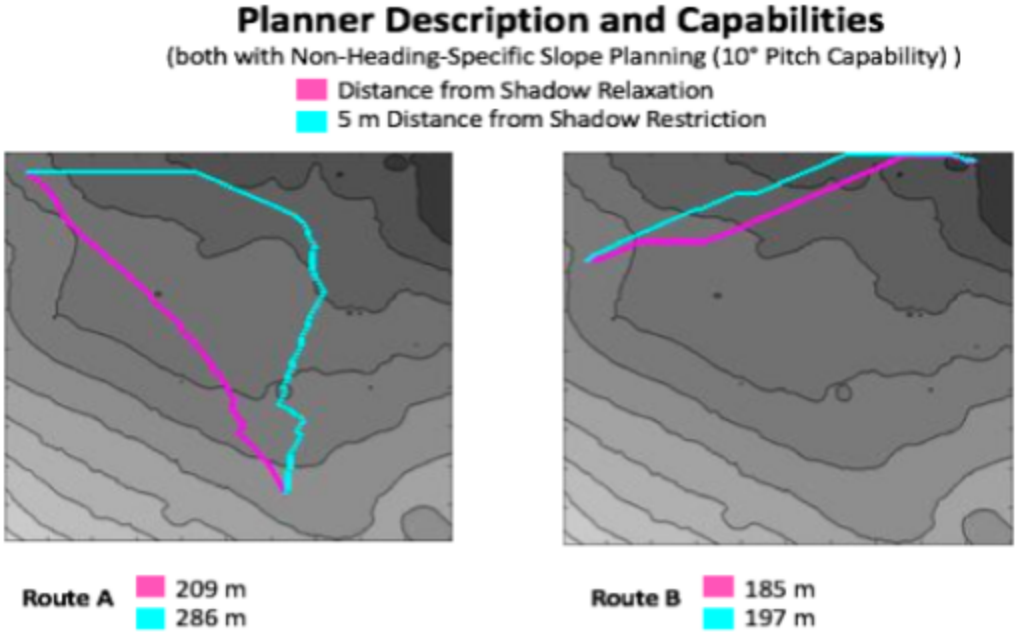

Fig. 24: A relaxed and restricted rover planning two different routes

Variance in distance from shadow restrictions were subsequently explored. Four rovers of varying distance from shadow restrictions were simulated in Fig. 25(a and b). Varying the restriction by a unit change of 5m does not significantly alter the path routes. The greatest change is seen in the highest restriction. Limitations, however, may be due to terrain navigability of non-heading-specific slope planning.

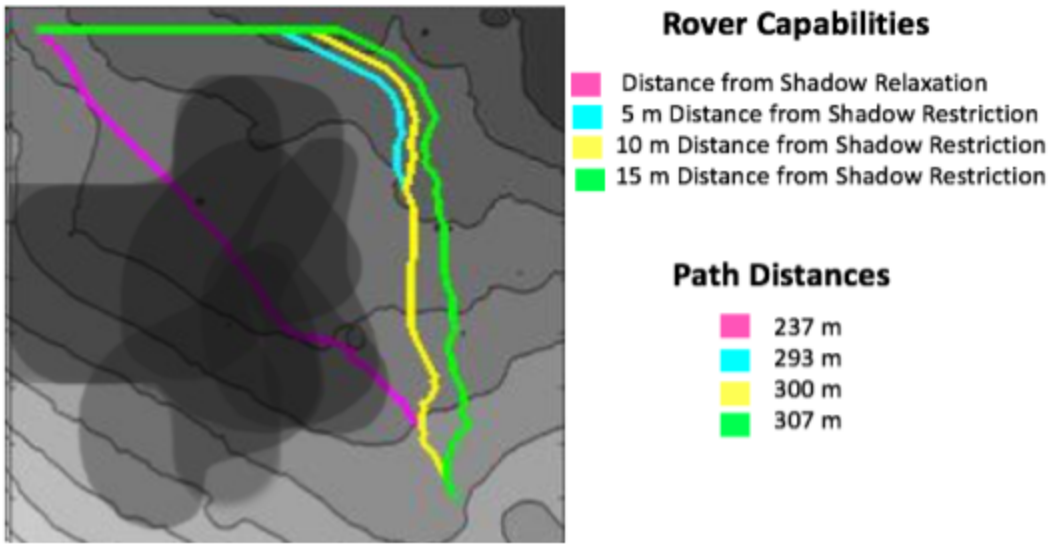

Fig. 25a: Four rovers with varying restrictions on distance from shadow planning a route (shadow intervals shown)

4.3 Varying Capabilities

Simulations of the distance from shadow restriction were applied to rovers with heading-specific slope planning. This was done on the modeled southwestern Nobile rim because of the terrain slope features as well as illumination qualities previously mentioned. As seen in Fig. 26, routes A and B both show that even with a distance from shadow restriction, rovers with heading-specific slope planning outperform non-heading-specific slope planning.

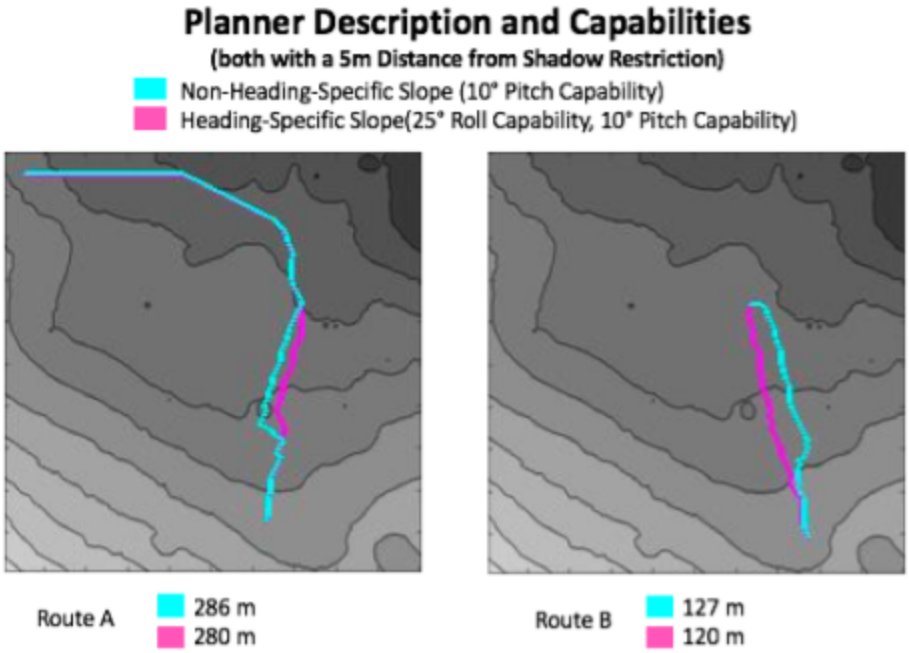

Fig. 26: Two distance from shadow restricted rovers with different planners on two different routes

Fig. 27 shows four rovers being simulated with varying capabilities. The rovers combined the two factors explored for path planning consideration: heading-specific slope planning and distance from shadow restriction. Heading-specific slope planning maintains shorter paths. Optimal rover selection was indeterminable as rationale for waypoint selection was based on feasibility for all four routes.

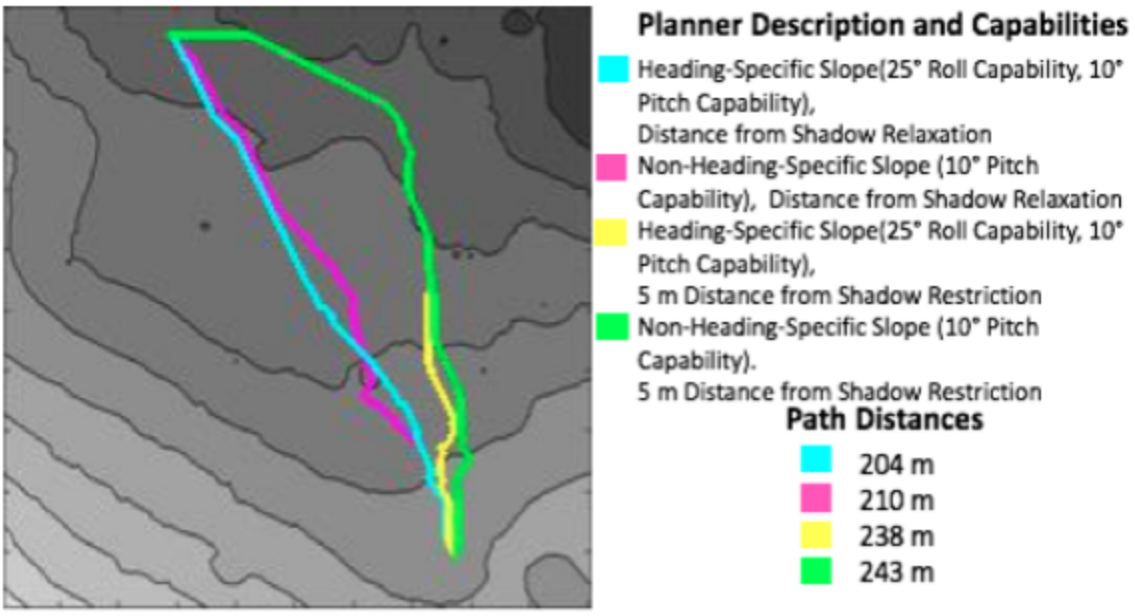

Fig. 27: Four rovers with different planner and constraints planning a route

4.4 Random Waypoint Generation

Random waypoint pairs were generated for each simulated site to compare heading-specific slope route generation to non-heading-specific slope route generation. Random start and end waypoints, map pixels, were randomly generated and considered a valid pair if the distance between the two points were over 50 m (1 meter per pixel) . A total of fifteen simulations were run for each site: generated hill, generated complex terrain, northwestern rim of Nobile, western rim of Nobile, and the southwestern rim of Nobile with distance from shadow restrictions (Fig. 28, Fig 29). For these simulations, whenever the non-heading-specific slope planner was able to generate a route, the heading-specific slope planner was also able to find a route. The comparison of these routes show that the heading-specific slope planner was able to find routes that were either shorter or equal in length to the non-heading-specific route (Fig. 30). Further, this shows that a majority of routes were only possible with heading-specific slope planning that would be impossible with non-heading-specific slope planning.

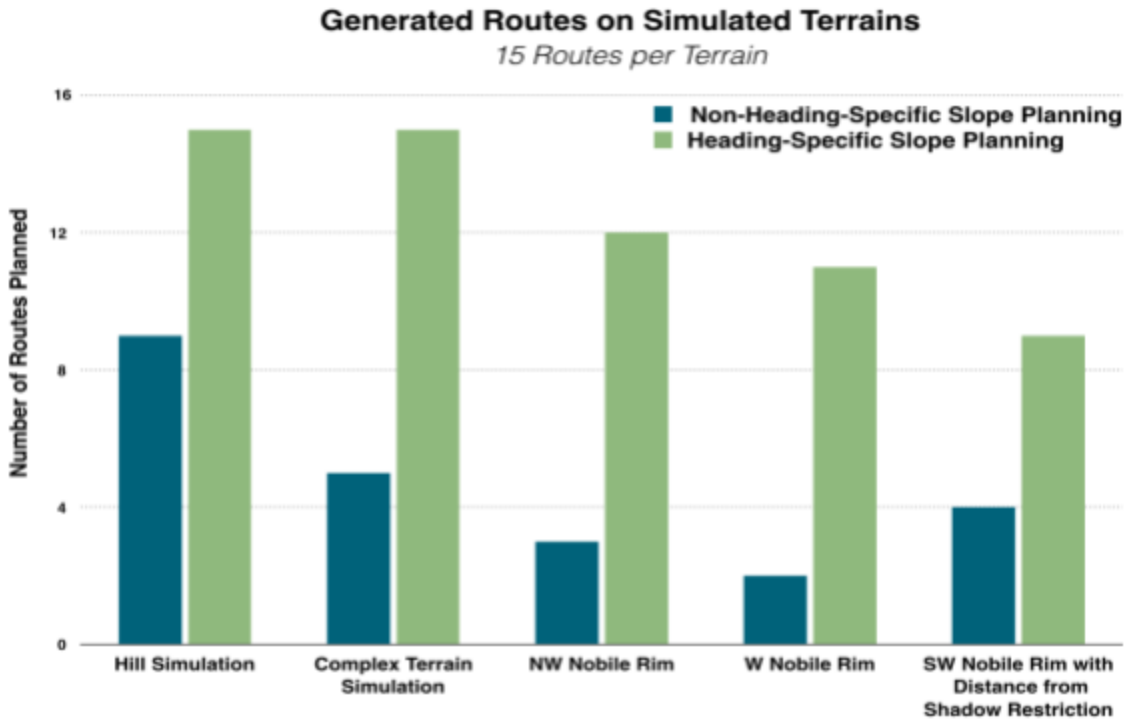

Fig. 28: A breakdown of route generation completion for fifteen randomly generated waypoints for each terrain

Generated Routes on Simulated Terrains (Percentage)

15 Routes per Terrain

	Hill Simulation	Complex Terrain Simulation	NW Nobile Rim	W Nobile Rim	SW Nobile Rim with Distance to Shadow
Non-Heading-Specific Slope	60%	33%	20%	13%	27%
Heading-Specific Slope	100%	100%	80%	73%	60%

Fig. 29 A percentage of successfully planned routes for 15 random generated waypoint combinations

Comparing Simulated Distance Traveled between Heading-Specific Slope Planning and Non-Heading Specific Slope Planning on Planned Routes

15 Routes per Terrain

	Hill Simulation	Complex Terrain Simulation	NW Nobile Rim	W Nobile Rim	SW Nobile Rim with Distance to Shadow
Same Length	33%	20%	0%	0%	0%
Shorter Length	67%	80%	100%	100%	100%

Fig. 30: This shows a comparison of calculated path lengths for when both the bearing-specific slope planner and non-bearing-specific slope planner generated routes for the random waypoint combinations

An additional set of random waypoint pairs(hundred simulated pairs) were generated for each simulated site to compare heading-specific slope route generation to non-heading-specific slope route generation (Fig. 31). This simulation was to see how much more area was possible to explore with heading-specific slope planning. On the northwestern Nobile Rim exploration increased by 69%, 41% on the western rim, and 37% on the southwestern rim.

Generated Routes on Simulated Terrains (Percentage)

100 Routes per Terrain

	NW Nobile Rim	W Nobile Rim	SW Nobile Rim
Non-Heading-Specific Slope	39%	51%	45%
Heading-Specific Slope	66%	72%	62%
Percent Improvement	69%	41%	37%

Fig. 31: Simulated terrain exploration (percentage) for Non-Heading-Specific Slope planning and Heading-Specific Slope planning.

A simulation of fifty routes were done to compare the effect of a distance from shadow constraint on path length (FIg. 32). All routes were tested on the same subsection of the southwestern rim. A simulation was only considered valid when all distance from shadow constraints were able to plan a route. The amount of routes unable to plan as the distance from shadow constraint was unexplored. With no constraint to remaining in illumination, the path length increased by 15.4%. With a 5m constraint, route length rose by 25.1%. For 10m and 15m distance from shadow constraint, path length increased by 30.8% and 38.7% respectively.

Generated Routes with Distance from Shadow

50 Routes per Terrain (Non-Heading-Specific Slope)

	No Distance from Shadow Consideration	Remain in Illumination	5m Distance from Shadow	10m Distance from Shadow	15m Distance from Shadow
Path Length Average *(Rounded to closest meter)*	227m	262m	284m	297m	315m
Path Length Increase (%) Compared to No Distance from Shadow Consideration	n/a	15.4%	25.1%	30.8%	38.7%

Fig. 32: A comparison of path length with varying distance from shadow constraints. Length and percentage increase are shown.

5. Discussions

This research shows that heading-specific slope planning enables routes that are not possible with non-heading-specific slope planning. Furthermore, while non-heading-specific slope planning works, heading-specific slope planning still has a route closer to the euclidean shortest distance. Distance from shadow constraints greatly alter planned paths. This buffer can maintain sun-synchronous planning, but does not account for encroaching shadow borders that occur in the illumination map's time interval. Adding these factors enables rovers to plan to certain waypoints with completely different paths when necessary.

5.1 Mission Scope

The only lunar area that was examined in this research was the western rim of Nobile. Another area that would be useful for heading-specific slope planning and distance from shadow would be Malapert. The site has two peaks illuminated at very low angle incidence. In exploration outside of lunar scenarios, heading-specific slope planning would be useful on Mars, specifically the Martian Recurring Slope Lineae (RSL) for proximity to observe. The RSL are dark markings along the surface of steep slopes on Mars thought to be caused by seasonal flows of briny water and are the most promising in search of life.

6. Conclusions

6.1 Summary

Heading-specific slope planning as well as distance from shadow constraints were implemented. Heading-specific slope planning was tested on simulated craters, hills, complex terrain, as well as Nobile's northwestern, western, and southwestern rim. It was demonstrated that heading-specific slope planning leads to paths that were not possible with non-heading-specific slope planning. If it was possible, the route is shorter with heading-specific slope planning on long routes. Distance from shadow constraints were tested on Nobile's southwestern rim. It was demonstrated that this restriction significantly altered planned route, increasing the route length in most cases. However, since charge is maintained with solar exposure, optimality could not be measured.

6.2 Conclusion

Because missions typically limit rover pitch capabilities to ensure safety, some destinations that are possible to reach by side sloping are not reachable by planning with max slope . There are planners that use finite difference of a given coordinate to its eight-connected neighbors limits node exploration to a scalar maximum slope value independent of the direction of that slope. Heading-specific slope planning was shown to reach destinations impossible with maximum slope planners. Furthermore, planning with directionality produced routes that were all of shorter or equal length. For successfully planned routes on hill and complex terrain simulation, heading-specific slope planning produced 66% and 80% of its routes to be of a shorter path length respectively. Furthermore, all routes on Nobile were shorter with heading-specific slope planning. This research's focus on slope directionality considerations for planning is not only applicable on lunar sites, but on any planetary exploration destination, including Mars, as those locations have terrain features that would exceed rover pitch limitations.

Traveling on a shadow boundary is possible with sun-synchronous navigation. Remaining in lit nodes is a weak constraint because of illumination map uncertainties and encroaching shadows. Planning with a distance from shadow ensures that there is a buffer. Traveling with a 0 m restriction produces the same routes as just traveling among lit nodes. Any stronger constraint further ensures a higher certainty of solar exposure.However, the focus on distance to shadow restrictions holds more applicability in areas with grazing incidences of light. This aspect subsequently holds more benefits on polar areas and therefore lunar rovers predominantly.

6.3 Future Work

A battery model should be implemented to consider the benefits of risk-aversion. The only heading-specific slope planning cost is the distance traveled to drive in that direction. Factors such as slope angle drains the rovers' batteries at different rates, depending on angle. As the roll and pitch capability to traverse a terrain increases, more battery is required to ascend. Furthermore, slope descent requires less battery than slope ascent. Longitudinal and lateral slip can be factored into planning that considers pitch and roll. Slip on terrain is not uniform, as varying roll and pitch capabilities impact respective slip rates.

To measure the benefits of distance from shadow, the planner should integrate a battery model that factors in solar charge. This would note if varying restrictions and relaxations allow the rover to accomplish routes before depleting charge. Strength of the solar flux is also not accounted for due to limitations of lighting maps. The lighting maps are binary for locations, and also do not take into the account the angle by which the rover charges. Solar panels may not be charge if the rover is at a certain slope.

There is no consensus as to the best metric for risk optimality. However, there has been much development in probabilistic risk modeling by Masahiro Ono (Ono, Williams & Blackmore, 2014). A probabilistic model that determines path selection based off path length as well as battery charge could utilized. This could be to create different types of risk models, depending on rover combinations. Different risk levels would be dependant on rover combination pairs, such as two independent rovers or a "risky" rover and a "safe" rover.

7. Bibliography

Cunningham, C. , Jones, H.L. , Kay, J., Peterson, K.M., and Whittaker, W.L., "Time-Dependent Planning for Resource Prospecting", Proceedings of the 12th International Symposium on Artificial Intelligence, Robotics, and Automation in Space, June, 2014.

Cunningham, C., Amato, J., Jones, H. L. and Whittaker, W. L. (2017) 'Accelerating Energy-Aware Spatiotemporal Path Planning for the Lunar Poles', in IEEE Conference on Robotics and Automation.

Dijkstra, E. W., "A note on two problems in connexion with graphs" Numerische Mathematik, 1(1):269–271, December 1959

Even, S., "Graph Algorithms" Cambridge University Press, 2011

Furlong, M., “Model Predictive Control for a Vehicle With an Actively Reconfigurable Chassis”, MS thesis, CMU-RI-TR-09-XX, April, 2009

Hart, P.E., Nilsson, N.J., and Raphael B., “A Formal Basis for the Heuristic Determination of Minimum Cost Paths”. IEEE Transactions on Systems Science and Cybernetics, 4(2):100–107, July 1968.

Haslum P. & Geffner H., “Admissable Heuristics for Optimal Planning”. AIPS 2000 Proceedings, pages 140–149, March 2000.

Helmick, D., Angelova, A., and Matthies, L., Terrain Adaptive Navigation for Planetary Rovers, Journal of Field Robotics, Vol.26, Issue 4, pp.391–410, 2009.

Howard, A., Seraji, H., and Werger, B. “A Terrain-Based Path Planning Method for Mobile Robots”, Proceedings of the 2002 IEEE International Conference, 2002

Iagnemma, K., Rzepniewski, A., Dubowsky, S., Pirjanian, P., Huntsberger, T., and Schenker, P.S., “Mobile robot kinematic reconfigurability for rough-terrain”, 2000.

Inotsume, H., “Analysis of Angle of Attack for Efficient Slope Ascent by Rovers”, M.S. thesis, CMU-RI-TR-15-22, August 2015

Inotsume, H., Creager, C., Wettergreen, D., and Whittaker, W. L., “Finding Routes for Efficient and Successful Slope Ascent by Exploration Rovers”, The International Symposium on Artificial Intelligence, Robotics and Automation in Space (i-SAIRAS), 2016.

Jet Propulsion Lab, “SRR: Sample-Return Rover.” Robotics Systems, https://www-robotics.jpl.nasa.gov/systems/systemImage.cfm?System=6&Image=108

Karumanchi, S., Allen, T., Bailey, T. and Scheding, S., “Non-Parametric Learning to Aid Path Planning over Slopes, The International Journal of Robotics Research, Vol.29, No.8, pp.997–1018, 2010.

Kohanbash, D.. “Scarab.” Lunar Rover, CMU Field Robotics Center, http://www.frc.ri.cmu.edu/projects/lri/scarab/images/MK_rover/IMG_1860.JPG.

Kohanbash, D., Conversation, March, 2017

Lemus, D. L. de M., Kohanbash, D., Moreland, S., and Wettergreen, D., “Slope Descent using Plowing to Minimize Slip for Planetary Rovers”, Journal of Field Robotics, Vol.26, Issue 6, pp.391–410, 2009.

McGhee, R. B. & Frank, A. A.,“On the stability properties of quadruped creeping gaits,” Math. Biosci., vol. 3, no. 3, pp. 331–351, 1968.

Nakamura, S., Faragalli, M., Mizukami, N., Nakatani, I., Kunii, Y., & Kubota, T. , “Wheeled robot with movable center of mass for traversing over rough terrain.”, In Proceedings of the 2007 IEEE/RSJ IROS, 2007.

NASA, “Lunar Reconnaissance”, https://www.nasa.gov/mission_pages/LRO/multimedia/lroimages/20100513_bullialdus.html, 2010

NASA, “Ice on the Moon: A Summary of Clementine and Lunar Prospector Results”, https://nssdc.gsfc.nasa.gov/planetary/ice/ice_moon.html, 2012

Ono, M., Williams, B. C., and Blackmore, L.. “Probabilistic planning for continuous dynamic systems under bounded risk”. Journal of Artificial Intelligence Research 46:511–577. 2013

Otten, N. D., Jones, H. L., Wettergreen, D. S. and Whittaker, W. L. (2015) ‘Planning routes of continuous illumination and traversable slope using connected component analysis’, 2015 IEEE International Conference on Robotics and Automation (ICRA), pp. 3953–3958. doi: 10.1109/ICRA.2015.7139751.

Phillips, M., Likhachev, M., and Koenig, S., “PA*SE: Parallel A* for Slow Expansions”. In Proceedings of the International Conference on Automated Planning and Scheduling (ICAPS), 2014.

Sanders, G., Moore, L., Mckay, D. et al. Regolith & Environment Science , and Oxygen & Lunar Volatile Extraction (RESOLVE) for Robotic Lunar Polar Lander Mission. In International Lunar Conference, pages 1–16, Toronto, Canada, 2005.

Schenker, P. S., Pirjanian, P., Balaram, B., Ali, K. S., Trebi-ollennu, A., Hunts- berger, T. L., Kennedy, H. Aghazarian B. A., Baumgartner, E. T., Rzepniewski, A., & Dubowsky, S., “Reconfigurable robots for all terrain exploration.”, Massachusetts Institute of Technology,, 2000.

Sefton-Nash, E., Siegler, M.A., and Paige, D.A., “Thermal Extremes in Permanently Shadowed Regions at the Lunar South Pole”, Proceedings of the 44th Lunar and Planetary Science Conference, March 2013.

Shillcut, K., “Solar Based Navigation for Robotic Explorers,” Ph. D. thesis, CMU-RI-TR-00-25, October 2000.

Tarokh, M. & McDermott, G., “Kinematics modeling and analyses of articulated rovers”, University of California - San Diego, Tech. rept. CS/10/2005. 2005

i.

Tarokh, M. & McDermott, G. “A Systematic Approach to Kinematics Modeling of High Mobility Wheeled Rovers”, IEEE International Conference on Robotics and Automation, p. 4905–4910, April 2007

Teti, F. , Whittaker, W. L., Kherat, S., Barfoot, T., and Sallaberger, C.,“Sun-Synchronous Lunar Polar Rover as a First Step to Return to the Moon”, International Symposium on Artificial Intelligence, Robotics and Automation in Space (iSAIRAS), 2005

Tompkins, P., Stentz, A., and Whittaker, W. L.,“Mission Planning for the Sun-Synchronous Navigation Field Experiment”, Proceedings of the 2002 IEEE International Conference on Robotics and Automation, May, 2002.

Tompkins, P. D., “Mission-Directed Path Planning for Planetary Rover Exploration”,. PhD thesis, CMU-RI-TR-05-20, May 2005

Vasavada, A. R., Bandfield, J. L., Greenhagen, B. T., Hayne, P. O., Siegler, M. A., Williams, J.P. , and Paige, D. A. ,“Lunar equatorial surface temperatures and regolith properties from the diviner lunar radiometer experiment,” Journal of Geophysical Research, vol. 117, 2012

Weisstein, Eric W, "Conical Spiral." From *MathWorld*--A Wolfram Web Resource, http://mathworld.wolfram.com/ConicalSpiral.html

Wellington, C., Courville, A., and Stentz, A., “A Generative Model of Terrain for Autonomous Navigation in Vegetation”, The International Journal of Robotics Research, Vol. 25, No. 12, pp. 1287 - 1304, December, 2006

Wettergreen, D., Dias, M. B., Shamah, B., Teza, J, Tompkins, P., Urmson, C., Wagner M. D.. and Whittaker, W. L.,"First Experiment in Sun-Synchronous Exploration", International Conference on Robotics and Automation May, 2002

Wettergreen, D., Jonak, D., Kohanbash, D., Moreland, S. J., Spiker, S., Teza, J., and Whittaker, W. L., "Design and Experimentation of a Rover Concept for Lunar Crater Resource Survey", 47th AIAA Aerospace Sciences Meeting including The New Horizons Forum and Aerospace Exposition, Aerospace Sciences Meetings, 2009

Whittaker, W. L., Kantor, G., Shamah, B., and Wettergreen, D., "Sun-Synchronous planetary exploration", in AIAA Space, 2000.

Ziglar, J."Rover Configuration for Exploring Lunar Craters", CMU-RI-TR-07-42, Robotics Institute, Carnegie Mellon University, December, 2007

Ziglar, J., Kohanbash, D., Wettergreen, D., and Whittaker, W. L.,"Technologies Toward Lunar Crater Exploration", CMU-RI-TR-07-40, Robotics Institute, Carnegie Mellon University, April, 2007

Ziglar, J., Kohanbash, D., Wettergreen, D., and Whittaker, W. L., "Plowing for Controlled Steep Crater Descents", International Symposium on Artificial Intelligence, Robotics and Automation in Space (iSAIRAS), February, 2008